

CHAPTER 4

F + H₂ REACTIVE SCATTERING

4.1 Introduction

Ever since the pioneering work of Polanyi and co-workers on atom + diatom reactive collision dynamics,¹⁻³ there has been an intense interest in reactive scattering on $F + H_2 \rightarrow HF(v, J) + H$ from the chemical physics community.⁴ The reasons for strong theoretical interest in this fundamental chemical reaction are readily appreciated. First of all, the $F + H_2$ system is an excellent prototype of a low barrier exothermic chemical reaction, yet small enough in total electron number and nuclear degrees of freedom to be tractable via high level *ab initio* calculations. This has led to the development of several potential energy surfaces,⁵⁻¹⁰ which has facilitated detailed classical,^{11,12} and quasi-classical¹³⁻¹⁵ studies of the $F + H_2$ reaction dynamics, as well as prediction of electron energy distributions from $[FH_2]^+$ photo detachment studies.^{16,17} Most importantly, there have been breakthroughs in three atom quantum reactive scattering that make feasible a numerically *exact* treatment of the reaction dynamics for a given adiabatic potential surface.¹⁷⁻²¹ As a

result, $F + H_2$ has evolved to become the “benchmark” chemical reaction system with which to compare experiment against theory at a fully rigorous level.

This theoretical interest has been stimulated by corresponding experimental efforts. Arrested relaxation methods of Polanyi and co-workers were first used to probe the $HF(v, J)$ rotational distributions via low pressure FTIR chemiluminescence methods.¹ Due to long residence times in the FTIR detection region, however, substantial collisional redistribution of the nascent HF product could occur; thus, “nascent” rovibrational distributions were estimated by extrapolation to the zero pressure limit. Crossed molecular beam methods by both Lee and co-workers at Berkeley²²⁻²⁴ and Toennies and co-workers at Goettingen²⁵⁻²⁷ have been used to investigate the *differential* reactive scattering of $F + H_2$ and isotropic variants for a series of center-of-mass collision energies. Due to limited energy resolution in these time-of-flight studies, however, only vibrational product levels could be resolved, with limited information on HF rotational distributions inferred from contour analysis. There has recently been a report from the Keil group of a measurement based on HF chemical laser excitation and bolometric detection that provides angularly resolved reactive scattering information on a single HF product quantum state.²⁸

The thrust of this chapter is to report a new IR laser based method for obtaining nascent product state distributions from $F + H_2$ under single collision conditions. Our approach is based on the following combination: i) A pulsed supersonic discharge source of F atoms is collided with a second pulsed jet source of H_2 molecules under sufficiently low densities to ensure single collision,

molecular beam conditions; ii) the product HF(v, J) is probed in the intersection region by high sensitivity direct absorption of a single mode tunable IR laser; and iii) as a function of laser tuning, these spectral data yield Doppler limited absorbance profiles on reactively scattered product HF(v, J) with complete resolution of final vibration/rotation quantum state. A complete description of the experimental method and results will be presented elsewhere;²⁹ this communication focuses on the highest vibrational manifold [i.e., HF($v=3, J$)] that is energetically accessible at 1.8(2) kcal/mol center of mass collision energy, E_{com} .

Such results provide the first opportunity for a fully rigorous comparison with exact quantum theoretical predictions of reactive scattering by Castillo and Manolopoulos²¹ on the lowest adiabatic F + H₂ potential energy surface of Stark and Werner.¹⁰ The agreement is found to be reasonably good, but theory substantially under predicts the high J rotational distributions near the energetic upper limit. These data provide indications that nonadiabatic channels involving both ground F(²P_{3/2}) and spin orbit excited F*(²P_{1/2}) atoms may be participating in the reaction dynamics.

4.2 Experiment

The experimental apparatus for state-to-state *reactive* scattering of F + H₂ is based on a modification of our earlier apparatus for state-to-state *inelastic* scattering, and is depicted schematically in figure 4-1. A pulsed discharge is used to generate high densities of F atoms upstream of the limiting expansion orifice (800 μm diameter) of an axisymmetric super-sonic jet. The stagnation gas is 5% F₂ in He obtained from a commercial excimer laser gas premix. The discharge is struck by

negatively biasing the orifice with respect to the valve body by ≈ 600 V, which results in 35 mA currents stabilized by a 5 k Ω ballast resistor in series with the discharge. Pulsed timing circuits are used to confine the discharge to a 200 μ s window near the peak of the full gas pulse (800 μ s). The H₂ supersonic jet is formed through a 200 μ m diameter pinhole with a piezoelectric actuator based on the design of Proch and Trickl.³⁰

Quantum state-resolved reactive scattering via direct IR laser absorption

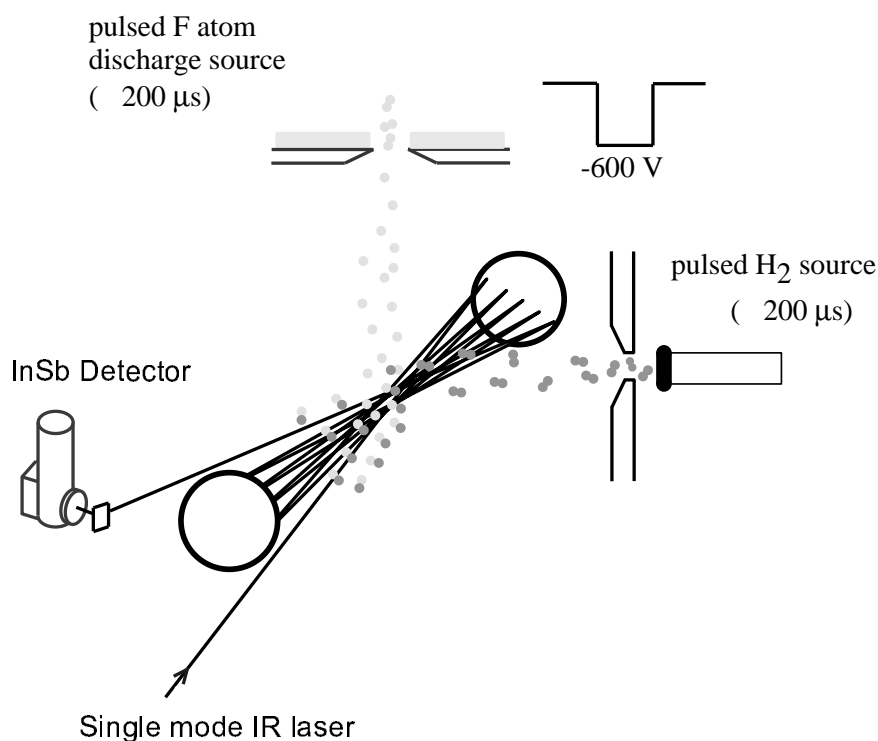


Figure 4-1. Schematic diagram of the crossed jet direct absorption reactive scattering experiment. Fluorine atoms produced in a discharge pulsed jet expansion are intersected at a 90° angle 4.5 cm downstream with a pulse of supersonically cooled H₂. Tunable single mode IR laser light is multi-passed perpendicular to the collision plane and probes HF(v , J) products by direct absorption.

The column integrated number density of H₂ in the intersection region is directly calibrated in a separate experiment by doping CH₄ into the stagnation gases at ≈1% level, and then monitoring direct IR absorption on the ν₃ CH stretch absorption band. Boltzmann analysis of the CH₄ rotational distribution estimates the rotational temperature of the H₂ reagent to be <30 K. Even at 100 K, H₂ is cooled essentially completely down into its lowest nuclear spin allowed states, namely $j=1$ (ortho) and $j=0$ (para) in a 3:1 ratio, with the first excited para ($j=2$) and ortho ($j=3$) states down 100- to 1000-fold.

The jets intersect 4.5 cm downstream of the nozzles, where for a typical 200 Torr H₂ backing pressure, the F atoms have a reaction probability of only ≈2%. Thus the probability of secondary inelastic collisions of the reaction products can be neglected, as explicitly verified by H₂ stagnation pressure studies. The temporal evolution of both gas pulses is monitored with miniature hearing aid microphones mounted inside the vacuum chamber on translational stages; time delay studies of the gas pulses are used to measure the velocity distributions for each beam. The H₂ and F atom beam velocities are $2.47(13) \times 10^5$ cm/s and $1.45(7) \times 10^5$ cm/s, respectively, which for the right angle collision geometry translates into $E_{\text{com}} = 1.8(2)$ kcal/mol. The 0.2 kcal/mol uncertainty arises predominantly from the finite spread in collision angles and is experimentally determined from Doppler profiles and Monte Carlo modeling. This energy width is more than threefold smaller than the rotational energy spacing between $J = 4$ and 5, and thus has a negligible effect on the product state distributions. The center-of-mass collision energy is essentially

equal to the 1.84 kcal/mol value used in previous quantum calculations of Castillo and Manolopoulos, which forms the basis of all comparison with theory in this chapter. The HF(v, J) reaction products are probed by direct absorption of a single mode color center laser that is multi-passed 16 times through the intersection region in a cylindrical Herriot cell.³¹ Absorption measurements are performed on the $\Delta v = +1$ fundamental HF band, and measure population *differences* between the upper and lower levels. Shot-noise limited absorption sensitivity is achieved by a combination of i) dual beam differential detection on matched InSb detectors and ii) electro-optic servo loop control of the color center laser intensity. All HF product signals are monitored on $\Delta v = +1$ *P* or *R* branch transitions, the frequencies for which are well determined and measured with a traveling wave meter of the Hall and Lee design.³² This yields readily detectable HF signals at 10^{-5} absorbance levels, which translate into sensitivities of $<1 \times 10^8$ /cm³/quantum state.

4.3 Results and Analysis

For each rotationally resolved transition, the time resolved HF signals are captured by a transient digitizer, integrated over the pulse duration, and stored on computer as a function of laser detuning. Sample results for *J*-dependent absorption signals in the HF($v = 3, J$) manifold are shown in figure 4-2, demonstrating velocity resolved Doppler profiles for the nascent HF product. Since this is a coherent absorption measurement, the HF($v = 3, J$) signals rigorously reflect population *differences* between the upper and lower rovibrational states. However, HF ($v = 4, J=0$) is energetically inaccessible to both F and F* at $E_{\text{com}} = 1.8(2)$ kcal/mol; thus the $v=4 \leftarrow 3$ signals in figure 4.2 reflect pure absorbance due solely to optical excitation

out of the $\text{HF}(v = 3, J)$ manifold. These absolute absorbances are rigorously converted³³ to absolute population densities per unit velocity subgroup by the IR linestrengths experimentally measured by Setser and co-workers from chemiluminescence studies.³⁴ We restrict our focus in this paper on state resolved *integral* scattering cross sections obtained by integrating over all Doppler velocity components, this yields the absolute *column integrated* populations i.e., molecules/ cm^2) for a given final J state over the region sampled by the probe laser beam.³³

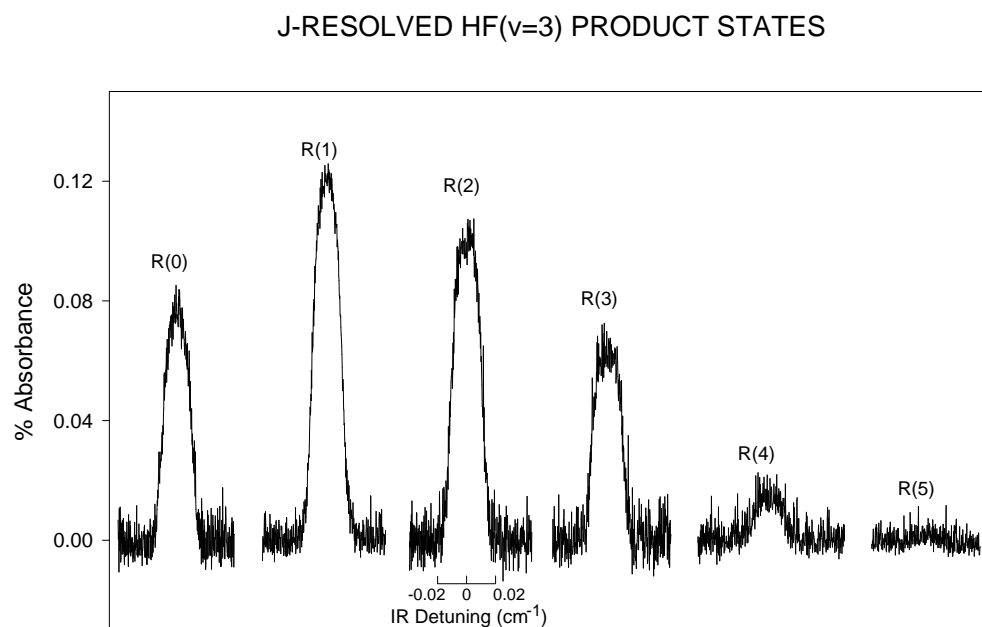


Figure 4-2. Sample absorption signals from $\text{HF}(v=3)$ produced by reactive scattering of F atoms with H_2 . Nascent population is evident in all J levels up to the energetic limit for the 1.8(2) kcal/mol center of mass collision energy.

4.4 Comparison with Theory

The highest level theoretical studies done to date on the $F + H_2(j)$ system have been the quantum reactive scattering calculations performed by Castillo and Manolopoulos,²¹ which predict differential and integral cross sections into given $HF(v, J)$ states on the lowest adiabatic potential surface of Stark and Werner.¹⁰ These differential cross sections can be related to the experimentally observed column integrated populations by center-of-mass to lab frame transformation. However, the resulting flux-to-concentration transformation between integral cross sections and populations for the current scattering geometry, kinematic mass combinations and energetics proves to be essentially independent of J . Thus to a very good approximation we can directly compare the experimental column integrated populations with the theoretical integral cross sections, averaged over the 1:3 nuclear spin distribution of $j = 0$ (para) and $j = 1$ (ortho) H_2 in the jet. This comparison is shown in figure 4-3, where the column integrated populations have been scaled to the integral cross section into $J = 1$. Overall the agreement between experiment and theory is quite good, with general trends in the experimental data well reproduced by theory. Agreement for the lower J values is especially quantitative, capturing the rise from $J = 0$ to nearly equivalent populations experimentally seen in $J = 1$ and 2. Given that these results are based on fully *ab initio* calculations and exact quantum scattering codes, this level of agreement serves to confirm the reliability of the Stark and Werner potential surface for this “bench-mark” atom + diatom reaction system. However, there are also substantial discrepancies between these theoretical predictions and experiment at higher J

values. Specifically, theory systematically *under-predicts* the populations in $J > 3$, by factors that greatly exceed the experimental uncertainty of the measurements. Indeed, the $J = 3$ experimental values are nearly two-fold larger than theoretically predicted, while this factor grows to nearly six-fold for $J = 4$. This effect is most dramatic in $J = 5$, which is an energetically closed channel on the Stark and Werner surface i.e., the integral cross section vanishes, whereas experimental signals clearly exist out to $J = 5$. Note that this is not plausibly due to finite resolution, since the energy difference between $J = 4$ and 5 is more than three-fold greater than experimental width in E_{com} .

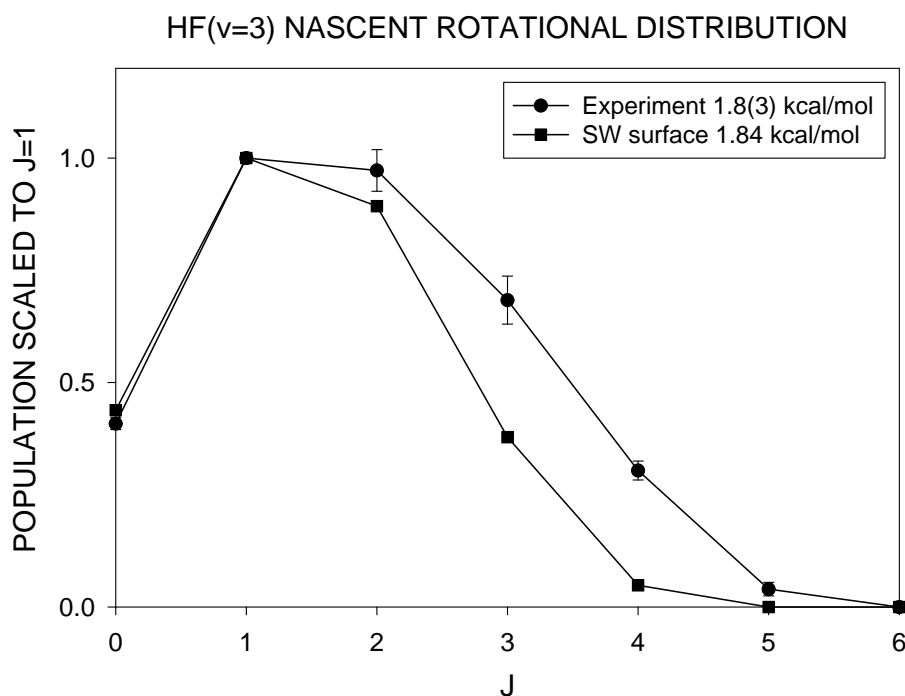


Figure 4-3. Nascent rotational distribution for $F + H_2 \rightarrow HF(v = 3) + H$ at $E_{\text{com}} = 1.8(2)$ kcal/mol (circles) compared to full quantum reactive scattering calculations (squares) by Castillo and Manolopoulos at 1.84 kcal/mol on the lowest adiabatic surface of Stark and Werner. Note the substantial underprediction of populations in $J \geq 3$.

As a final comment, it is worth speculating on what the high J discrepancies between experiment and theory might be due to. The quantum reactive scattering calculations of Castillo and Manolopoulos are “exact” for reactions on a given adiabatic potential surface; thus the simplest interpretation would be that these high J discrepancies may reflect deficiencies in Stark and Werner’s lowest adiabatic surface in the barrier region. Alternatively, it is possible that the $F + H_2$ reactions do not take place exclusively on the single lowest *adiabatic* potential surface, though this has been explicitly assumed in all $F + H_2$ quantum reactive scattering calculations thus far. If *nonadiabatic* effects are important, then one would also anticipate contributions to reactive scattering from low lying spin orbit excited $F^*(^2P_{1/2})$ atoms also present in the jet. Given the 1.16 kcal/mol (404 cm^{-1}) spin orbit splitting between F and F^* , this would help explain the excess population experimentally observed in $J > 3$. The intriguing possibility of nonadiabatic $F^* + H_2$ reaction pathways can be tested experimentally by lowering the center-of-mass collision energy below the energetic threshold for forming a specific $HF(v, J)$ product state from the purely adiabatic $F + H_2$ reaction channel. These and other threshold studies are currently being pursued in our laboratory.

References for Chapter 4

- 1 J. C. Polanyi and K. B. Woodall, *J. Chem. Phys.* **57**, 1574 (1972).
- 2 D. H. Maylotte, J. C. Polanyi, and K. B. Woodall, *J. Chem. Phys.* **57**, 1547 (1972).
- 3 F. E. Bartoszek, D. M. Manos, and J. C. Polanyi, *J. Chem. Phys.* **69**, 933 (1978).
- 4 D. E. Manolopoulos, *J. Chem. soc., Faraday Trans.* **93**, 673 (1997).
- 5 C. F. Bender, P. K. Pearson, S. V. O'Neil, and H. F. Schaefer III, *J. Chem. Phys.* **56**, 4626 (1972).
- 6 J. T. Muckerman, *J. Chem. Phys.* **56**, 2997 (1972).
- 7 R. Steckler, D. G. Truhlar, and B. C. Garrett, *J. Chem. Phys.* **82**, 5499 (1985).
- 8 T. Takayanagi and S. Sato, *Chem. Phys. Lett.* **144**, 191 (1988).
- 9 G. C. Lynch, R. Steckler, D. W. Schwenke, A. J. C. Varandas, and D. G. Truhlar, *J. Chem. Phys.* **94**, 7136 (1991).
- 10 K. Stark and H.-J. Werner, *J. Chem. Phys.* **104**, 6515 (1996).
- 11 R. L. Jaffe, J. M. Henry, and J. B. Anderson, *J. Chem. Phys.* **59**, 1128 (1973).
- 12 J. T. Muckerman, *J. Chem. Phys.* **57**, 3382 (1972).
- 13 W. Jakubetz and J. N. L. Connor, *Faraday Discuss. Chem. Soc.* **62**, 324 (1977).
- 14 D. Neuhauser, R. S. Judson, R. L. Jaffe, M. Baer, and D. J. Kouri, *Chem. Phys. Lett.* **176**, 546 (1991).
- 15 F. J. Aoiz, L. Banares, V. J. Herrero, V. Saez Rabanos, K. Stark, and H.-J. Werner, *J. Chem. Phys.* **102**, 10665 (1994).
- 16 S. E. Bradforth, D. W. Arnold, D. M. Neumark, and D. E. Manolopoulos, *J. Chem. Phys.* **99**, 6345 (1993).

- 17 D. E. Manolopoulos, K. Stark, H.-J. Werner, D. W. Arnold, S. E. Bradforth, and D. M. Neumark, *Science* **262** (1993).
- 18 J. Z. H. Zhang and W. H. Miller, *J. Chem. Phys.* **88**, 4549 (88).
- 19 J. M. Launay and M. Le Dourneuf, *Chem. Phys. Lett.* **169**, 473 (1990).
- 20 J. Z. H. Zhang, *Chem. Phys. Lett.* **181**, 63 (1991).
- 21 J. F. Castillo, D. E. Manolopoulos, K. Stark, and H.-J. Werner, *J. Chem. Phys.* **104**, 6531 (1996).
- 22 T. P. Schafer, P. E. Siska, J. M. Parson, F. P. Tully, Y. C. Wong, and Y. T. Lee, *J. Chem. Phys.* **53**, 3385 (1970).
- 23 D. M. Neumark, A. M. Wodtke, G. N. Robinson, C. C. Hayden, and Y. T. Lee, *J. Chem. Phys.* **82**, 3045 (1985).
- 24 D. M. Neumark, A. M. Wodtke, G. N. Robinson, C. C. Hayden, K. Shobatake, R. K. Sparks, T. P. Schafer, and Y. T. Lee, *J. Chem. Phys.* **82**, 3067 (1985).
- 25 M. Faubel, L. Rusin, S. Schlemmer, F. Sundermann, U. Tappe, and J. P. Toennies, *J. chem. Soc., Faraday Trans.* **89**, 1475 (1993).
- 26 M. Faubel, L. Y. Rusin, S. Schlemmer, F. Sundermann, U. Tappe, and J. P. Toennies, *J. Chem. Phys.* **101**, 2106 (1994).
- 27 Faubel, *Z. Phys. Chem.* **188**, 197 (1995).
- 28 G. Dharmasena, T. R. Phillips, K. N. Shokirev, G. A. Parker, and M. Keil, *J. Chem. Phys.* **106**, 9950 (1997).
- 29 W. B. Chapman, B. W. Blackmon, and D. J. Nesbitt, (in preparation).
- 30 D. Proch and T. Trickl, *Rev. Sci. Instrum.* **60**, 713 (1989).
- 31 D. Herriott, H. Kogelnik, and R. Kompfner, *Appl. Opt.* **3**, 523 (1964).
- 32 J. L. Hall and S. A. Lee, *Appl. Phys. Lett.* **29**, 367 (1976).
- 33 W. B. Chapman, M. J. Weida, and D. J. Nesbitt, *J. Chem. Phys.* **106**, 2248 (1997).
- 34 E. Arunan, D. W. Setser, and J. F. Ogilvie, *J. Chem. Phys.* **97**, 1734 (1992).